

Cite this: *J. Mater. Chem.*, 2012, **22**, 1191

www.rsc.org/materials

PAPER

## Mixed lanthanide succinate–sulfate 3D MOFs: catalysts in nitroaromatic reduction reactions and emitting materials†

Richard F. D'Vries,<sup>a</sup> Marta Iglesias,<sup>a</sup> Natalia Snejko,<sup>a</sup> Susana Alvarez-Garcia,<sup>ab</sup> Enrique Gutiérrez-Puebla<sup>a</sup> and M. Angeles Monge<sup>\*a</sup>

Received 20th September 2011, Accepted 26th October 2011

DOI: 10.1039/c1jm14677g

The first series of mixed succinate/sulfate/Ln MOFs,  $[\text{Ln}_2(\text{C}_2\text{H}_4\text{C}_2\text{O}_4)_2(\text{SO}_4)(\text{H}_2\text{O})_2]$  (**RPF-16**), where Ln = La, Pr, Nd, and Sm, were hydrothermally obtained and their structures determined by X-ray single crystal diffraction. The crystalline products are a series of isostructural 3D polymeric compounds that crystallise in the monoclinic space group  $P2(1)/n$ . Their framework comprises infinite crossing chains of  $\text{LnO}_9$  sharing edges polyhedra, kept together by succinate and sulfate anions. Topological simplification gives rise to a 3D uninodal six connected net of type **pcu alpha-Po** primitive cubic. These well-defined compounds show high chemoselectivity towards reduction of the nitro group and present bifunctional activity for the one-pot reductive amination of heptanal at near-complete conversion of the substrates. A general overview of the room-temperature luminescence behavior in the new **RPF-16** Ln materials is also reported.

## Introduction

The metal–organic frameworks that contain trivalent lanthanide cations are widely known for their uses as optical<sup>1,2</sup> and sensor materials,<sup>3</sup> in gases absorption,<sup>4</sup> as magnetic materials,<sup>5,6</sup> catalysts<sup>7–9</sup> and drug carriers.<sup>10</sup> The growing number of reports of applications of this kind of compounds in different fields depicts the importance of the lanthanide MOFs<sup>11</sup> in the development of new technologies. In the catalysis field, the Ln-MOFs are poorly used and few examples have been reported in epoxidation of olefins,<sup>12</sup> oxidation of organic sulfurs,<sup>13</sup> acetalization of aldehydes,<sup>14</sup> and some other reactions.<sup>2</sup> On the other hand, the sulfate anion is an effective component to built structures with new topologies, and materials with different properties.<sup>15</sup> Most of the reported works on lanthanide sulfates focus generally on inorganic structures containing alkali metal or ammonium ions.<sup>16,17</sup>

Concerning organic multidentate ligands (spacers) linking lanthanide ions (connectors), there is a good number of new compounds with very different and, in some cases, new topologies. However, the obtaining of new compounds combining  $\text{SO}_4$  anions

and nitrogen-free aliphatic linker remains still a challenge. Only a few lanthanide oxalate–sulfates have been reported,<sup>18–20</sup> and most of them own anionic frames with  $\text{NH}_4^+$  cations in their tunnels.

In the search for new architectures of lanthanide MOFs, and after a long time studying lanthanide sulfate, sulfonate and succinate compounds, as well as their material properties, in this work we present the first series of mixed succinate/sulfate/Ln MOFs,  $[\text{Ln}_2(\text{C}_2\text{H}_4\text{C}_2\text{O}_4)_2(\text{SO}_4)(\text{H}_2\text{O})_2]$  (**RPF-16**), where Ln = La, Pr, Nd, and Sm. These compounds were hydrothermally obtained and their structures determined by X-ray single crystal diffraction. Characterization of the bulk samples by powder X-ray diffraction, IR and thermogravimetric analysis is also reported. **RPF-16** series has been explored as potential chemoselective heterogeneous catalysts for the reduction of nitroarenes in the presence of other reducible functional groups. The materials were also tested as bifunctional catalysts for the one-pot reductive amination of heptanal. Additionally, a general overview of the room-temperature luminescence behaviour of the new **RPF-16** materials is reported.

## Experimental section

## General information

All reagents and solvents employed were commercially available and used as supplied without further purification: succinic acid (98% Merck); disodium sulfate (98% Merck); lanthanum nitrate hexahydrate (99.9% Alfa Aesar); praseodymium nitrate hexahydrate (99.9% Strem Chemicals); neodymium nitrate hexahydrate (99.9% Alfa Aesar); samarium nitrate hexahydrate (99.9% Strem Chemicals).

<sup>a</sup>Instituto de Ciencia de Materiales de Madrid (ICMM-CSIC), Cantoblanco, 28049 Madrid, Spain. E-mail: amonge@icmm.csic.es; Fax: +34 913720623

<sup>b</sup>Instituto Química-Física Rocasolano, (CSIC), Madrid, E-28006, Spain

† Electronic supplementary information (ESI) available: Experimental and simulated powder X-ray diffraction patterns, selected bond lengths, intramolecular hydrogen bonds, X-ray powder patterns after TG analysis and X-ray powder patterns after catalytic studies for compounds **1–4**. CCDC reference numbers 828893, 828894, 828895 and 828896. For ESI and crystallographic data in CIF or other electronic format see DOI: 10.1039/c1jm14677g

The IR spectra were recorded from KBr pellets in the range 4000–250  $\text{cm}^{-1}$  on a Bruker IFS 66V/S. The thermogravimetric and differential thermal analyses (TGA-DTA) were performed using Seiko TG/DTA 320U equipment in the temperature range between 25 and 1000  $^{\circ}\text{C}$  in air (100  $\text{mL min}^{-1}$  flow) atmosphere and a heating rate of 10  $^{\circ}\text{C min}^{-1}$ . A Perkin-Elmer CHNS Analyzer 2400 was employed for the elemental analysis. Powder X-ray diffraction (PXRD) patterns were measured with a Bruker D8 diffractometer, with a step size of  $0.02^{\circ}$  and exposure time of 0.5 s per step.

## Synthesis

The compounds were synthesized under hydrothermal conditions. The molar composition of the initial reaction mixture was  $0.5 \text{ SO}_4^{2-} : \text{Ln}^{3+} : \text{Succ}^{2-} : 1500 \text{ H}_2\text{O}$ .

$[\text{La}_2(\text{C}_2\text{H}_4\text{C}_2\text{O}_4)_2(\text{SO}_4)(\text{H}_2\text{O})_2]$  (**1**) was synthesized by addition of 0.027 g (0.231 mmol) of succinic acid and 0.016 g (0.115 mmol) of disodium sulfate to a dissolution of lanthanum nitrate hexahydrate (0.1 g, 0.231 mmol) in 6 mL of water with constant stirring for 15 minutes. The pH of the mixture was fixed at 5.0 (NaOH, 1  $\text{mol L}^{-1}$ ). The resultant reaction mixture was transferred to a Teflon-lined stainless steel autoclave and heated at 160  $^{\circ}\text{C}$  for 18 hours. Colourless crystals suitable for X-ray diffraction analysis were obtained by quenching the vessel, after being filtered and washed with water and acetone (yield 70%).

Compounds  $[\text{Ln}_2(\text{C}_2\text{H}_4\text{C}_2\text{O}_4)_2(\text{SO}_4)(\text{H}_2\text{O})_2]$  [ $\text{Ln} = \text{Pr}$  (**2**),  $\text{Nd}$  (**3**) and  $\text{Sm}$  (**4**)] were synthesized using a similar procedure; crystalline products **2** (light green, yield 75%), **3** (violet, yield 68%) and **4** (light yellow, yield 82%) were obtained by quenching the vessel, after being filtered and washed with water and acetone. Elemental analysis, calculated for **1** ( $\text{C}_8\text{H}_{12}\text{O}_{14}\text{SLa}_2$ ): C, 14.95; H, 1.87; S, 4.98; found: C, 14.64; H, 1.75; S, 5.18%; calculated for **2** ( $\text{C}_8\text{H}_{12}\text{O}_{14}\text{SPr}_2$ ): C, 14.86; H, 1.86; S, 4.95; found: C, 14.50; H, 1.76; S, 5.17%; calculated for **3** ( $\text{C}_8\text{H}_{12}\text{O}_{14}\text{SNd}_2$ ): C, 14.71; H, 1.84; S, 4.90; found: C, 14.37; H, 1.72; S, 4.30%; calculated for **4** ( $\text{C}_8\text{H}_{12}\text{O}_{14}\text{SSm}_2$ ): C, 14.44; H, 1.80; S, 4.81; found: C, 14.37; H, 1.77; S, 4.89%.

## Single-crystal structure determination

Single-crystal X-ray diffraction data for the compounds were obtained in a Bruker-Siemens Smart CCD diffractometer equipped with a normal focus, 2.4 kW sealed tube X-ray source (Mo  $\text{K}\alpha$  radiation = 0.71073  $\text{\AA}$ ) operating at 50 kV and 20 mA. Data were collected over a hemisphere of the reciprocal space by a combination of three sets of exposure. Each exposure of 20 s covered  $0.3^{\circ}$  in  $\omega$ . The unit cell dimensions were determined for Least-Square fit of reflections with  $I > 2\sigma$ . The structures were resolved by direct methods. The final cycles of refinement were carried out by full-matrix least-square analyses with anisotropic thermal parameters of all non-hydrogen atoms. The hydrogen atoms were fixed at their calculated positions using distances and angle constraints. All calculations were performed using SMART software for data collection,<sup>21</sup> SAINT for data reduction<sup>22</sup> and SHELXTL to resolve and refine the structure.<sup>23</sup>

## X-Ray powder diffraction

The X-ray powder diffraction measurements were used to check the purity of the obtained microcrystalline products by comparison of the experimental results with the simulated patterns obtained from single crystal X-ray diffraction data. The residues for the compounds after TG analyses were analysed by X-ray powder diffraction and compared with ICSD patterns reported.

## Optical measurements

Photoluminescence spectra of individual crystals were obtained at room temperature exciting with one line (488 nm) of an  $\text{Ar}^+$  laser, a Jobin-Yvon HR 460 monochromator, coupled to a  $\text{N}_2$  cooled CCD. The excitation light was focused on the sample with an Olympus microscope which is also used to collect the scattered light with 100 $\times$  objectives. The crystals were larger than the spot size (around 1 micron). Notch filters of the corresponding wavelengths were used to eliminate the elastic component of the collected light. The spectra were corrected by the instrumental function recorded with a calibrated white source and a  $\text{CaF}_2$  pellet.

## Catalytic reduction of nitroaromatic compounds

The catalytic properties in hydrogenation of nitroaromatic reactions of the **RPF-16** compounds were examined under conventional conditions for batch reactions in a reactor (Autoclave Engineers) of 100 mL capacity in toluene and 1/200 metal/substrate molar ratio,  $5 \times 10^5$  Pa of  $\text{H}_2$  pressure and at 363 K temperature. The nitro compound was dissolved in toluene and the catalyst (0.5 mol%) was added. The mixture was placed in an autoclave. After purging with  $\text{H}_2$  the reaction mixture was heated to the desired temperature and stirred (1500 rpm). The products composition was determined by means of gas chromatography; the reaction mixture was centrifuged for removing the catalyst. The products were identified by gas chromatography/mass spectrometry (GC-MS). Only experiments with mass balances >95% were considered.

## Results and discussion

Details of crystallographic data, data collection and refinement are summarized in Table 1. An ORTEP representation of the compounds is shown in Fig. 1.

Upon determining the crystal structure, the formula of these isostructural series of compounds turned out to be  $[\text{Ln}_2(\text{C}_2\text{H}_4\text{C}_2\text{O}_4)_2(\text{SO}_4)(\text{H}_2\text{O})_2]$ , (**RPF-16**), where  $\text{Ln} = \text{La}$ ,  $\text{Pr}$ ,  $\text{Nd}$ , and  $\text{Sm}$ . This structural type crystallizes in the monoclinic space group  $P2(1)/n$ . The lanthanide ion is coordinated to nine oxygen atoms: six of succinate ligands, two of different sulfate groups, and one of a water molecule in  $\text{LnO}_9$  tricapped trigonal prisms (Fig. 1 and S2, ESI<sup>†</sup>). The two crystallographically independent succinate anions (A and B) present in the structure have *trans* conformation. Averages of the torsion angle values for the four isostructural new compounds were made with the following results: ( $\text{C5C4C3C8}$ ) =  $176.5^{\circ}$  and ( $\text{C1C2C6C7}$ ) =  $163.6^{\circ}$  for (A) and (B) ligands, respectively. Concerning the carboxylate groups: the values are ( $\text{O8C5C4C3}$ ) =  $71.1^{\circ}$  and

**Table 1** Crystallographic data and refinement details for **RPF-16**

Compound	1	2	3	4
Empirical formula	C <sub>8</sub> H <sub>12</sub> O <sub>14</sub> SLa <sub>2</sub>	C <sub>8</sub> H <sub>12</sub> O <sub>14</sub> SPr <sub>2</sub>	C <sub>8</sub> H <sub>12</sub> O <sub>14</sub> SNd <sub>2</sub>	C <sub>8</sub> H <sub>12</sub> O <sub>14</sub> SSm <sub>2</sub>
FW	642.07	646.07	652.73	664.94
Temperature/K	298(2)	298(2)	298(2)	298(2)
Wavelength/Å	0.71073	0.71073	0.71073	0.71073
Crystal system	Monoclinic	Monoclinic	Monoclinic	Monoclinic
Space group	<i>P</i> 2 <sub>1</sub> / <i>n</i>	<i>P</i> 2 <sub>1</sub> / <i>n</i>	<i>P</i> 2 <sub>1</sub> / <i>n</i>	<i>P</i> 2 <sub>1</sub> / <i>n</i>
<i>Unit cell dimensions</i>				
<i>a</i> /Å	12.881(2)	12.7580(10)	12.7225(19)	12.6365(6)
<i>b</i> /Å	9.6559(16)	9.5881(8)	9.5748(14)	9.5308(4)
<i>c</i> /Å	13.088(2)	12.9304(11)	12.897(2)	12.8091(6)
$\beta$ /°	110.357(3)	110.2330(10)	110.205(2)	110.1280(10)
Volume/Å <sup>3</sup>	1526.2(4)	1484.1(2)	1474.4(4)	1448.46(11)
<i>Z</i>	4	4	4	4
$\rho$ calc/Mg m <sup>-3</sup>	2.794	2.891	2.941	3.049
Absorption coefficient/mm <sup>-1</sup>	5.736	6.707	7.186	8.253
<i>F</i> (000)	1208	1224	1232	1248
Crystal size	0.11 × 0.07 × 0.06	0.60 × 0.40 × 0.10	0.12 × 0.07 × 0.06	0.11 × 0.07 × 0.04
$\theta$ range for data collection/°	1.91 to 26.39	1.93 to 26.37	1.94 to 26.37	1.95 to 25.03
Reflections collected/unique	120 24/3091 [ <i>R</i> (int) = 0.0435]	11 810/3012 [ <i>R</i> (int) = 0.0351]	11 438/2977 [ <i>R</i> (int) = 0.0491]	10 285/2549 [ <i>R</i> (int) = 0.0436]
Completeness (%)	99.00%	99.50%	99.20%	99.40%
Data/restraints/parameters	3091/0/226	3012/0/226	2977/0/208	2549/0/236
Goodness-of-fit on <i>F</i> <sup>2</sup>	1.178	1.376	1.314	1.272
<i>R</i> 1 [ <i>I</i> > 2 $\sigma$ ( <i>I</i> )]	<i>R</i> 1 = 0.0343	<i>R</i> 1 = 0.0356	<i>R</i> 1 = 0.0696	<i>R</i> 1 = 0.0365
<i>wR</i> 2 [ <i>I</i> > 2 $\sigma$ ( <i>I</i> )]	<i>wR</i> 2 = 0.0731	<i>wR</i> 2 = 0.0907	<i>wR</i> 2 = 0.1961	<i>wR</i> 2 = 0.0821
<i>R</i> 1 (all data)	<i>R</i> 1 = 0.0471	<i>R</i> 1 = 0.0429	<i>R</i> 1 = 0.0836	<i>R</i> 1 = 0.0489
<i>wR</i> 2 (all data)	<i>wR</i> 2 = 0.0758	<i>wR</i> 2 = 0.0925	<i>wR</i> 2 = 0.2002	<i>wR</i> 2 = 0.0850
Largest diff. peak and hole	1.457 and −1.131	1.615 and −1.251	5.802 and −2.565	1.648 and −1.319

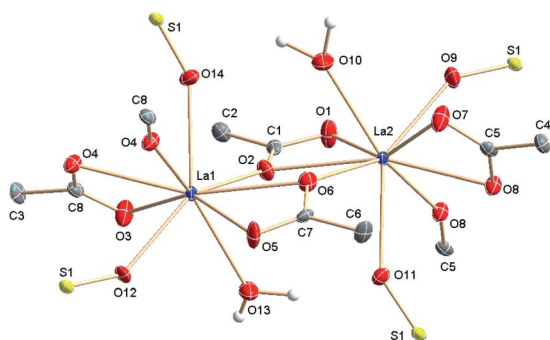


**Fig. 1** ORTEP drawing of the asymmetric unit for the **[La<sub>2</sub>(C<sub>2</sub>H<sub>4</sub>C<sub>2</sub>O<sub>4</sub>)<sub>2</sub>(SO<sub>4</sub>)(H<sub>2</sub>O)<sub>2</sub>]** compound; ellipsoids are displayed at the 50% probability level and some hydrogen atoms are omitted for clarity. Symmetry transformations used to generate equivalent atoms: (a)  $-x + 1, -y + 1, -z + 1$ ; (b)  $-x + 1, -y + 2, -z$ ; (c)  $-x + 3/2, y - 1/2, -z + 1/2$ ; (d)  $x + 1/2, -y + 3/2, z + 1/2$ ; (e)  $x - 1/2, -y + 3/2, z - 1/2$ ; (f)  $-x + 3/2, y + 1/2, -z + 1/2$ ; (g)  $x, y, z + 1$ ; (h)  $x, y, z - 1$ .

(O3C8C3C4) = 61.4° for (A) succinate, for (B) one is smaller, (O1C1C2C6) = 3.27° while the other is in the same order of those of (A): (O1C7C6C2) = 73.8°. These differences are due to the type of coordination and to the succinate flexibility, which allow the formation of the three-dimensional network. In both cases, the carboxylate anions are bound in the uncommon chelating bridge mode  $\eta_2\mu^2-\eta_2\mu^1$ , simplified as  $\mu^2:\mu^1:\eta_2$  (Fig. 2).

This arrangement gives rise to infinite chains of LnO<sub>9</sub> sharing edges polyhedra, with Ln1...Ln2 distances in the chain of (La1...La2) = 4.3817(8), (Pr1...Pr2) = 4.3327(8), (Nd1...Nd2) = 4.324 (1) and (Sm1...Sm2) = 4.2972(8) Å (ESI†, Fig. S2). These chains,

which run along the *b* and *c* directions in a crossing way, are joined by the sulfate group, which is coordinated to four different metallic centres at distances and angles corresponding to its tetrahedral conformation (ESI†, Fig. S2). In this way, a totally inorganic 3D net would be formed. Besides, there are other connections along the [100] and [101] directions, through the (B) and (A) succinate linkers, respectively. Additionally, two intramolecular hydrogen bonds between the coordination water and the oxygen atoms of the sulfate and carboxylate groups were found (ESI†, Fig. S3).

For topological study of the 3D net, after trying the rod-shape packing method<sup>24</sup> and in order to obtain the simplest net the model has been simplified as follows: the chain nodes were placed in the Ln...Ln distances middle points, so that SO<sub>4</sub> anions become bi-connected, and thus, they do not represent nodes, but linkers. Sulfate linkers play an essential role in the structure, since they join the crossing chains, forming the main scaffold. The succinate ligands are the other linkers that join the parallel chain centroids. As a result of this simplification, a 3D uninodal six connected net of type **pcu alpha-Po** primitive cubic is found (Fig. 2), with a point (Schläfli) symbol (4<sup>12</sup> × 6<sup>3</sup>), which agrees with the program TOPOS analysis.<sup>25</sup>

### Thermal stability study

All the compounds present similar decomposition curves (Fig. 3); the compounds are stable up to ~260 °C. Decomposition begins with the loss of coordinated water and follows with the total decomposition, losing the ligand molecule around ~500 °C (% water mass calculated: compound 1: 5.8; 2: 5.57; 3: 5.52; and 4: 5.41). Decomposition products for the four compounds were

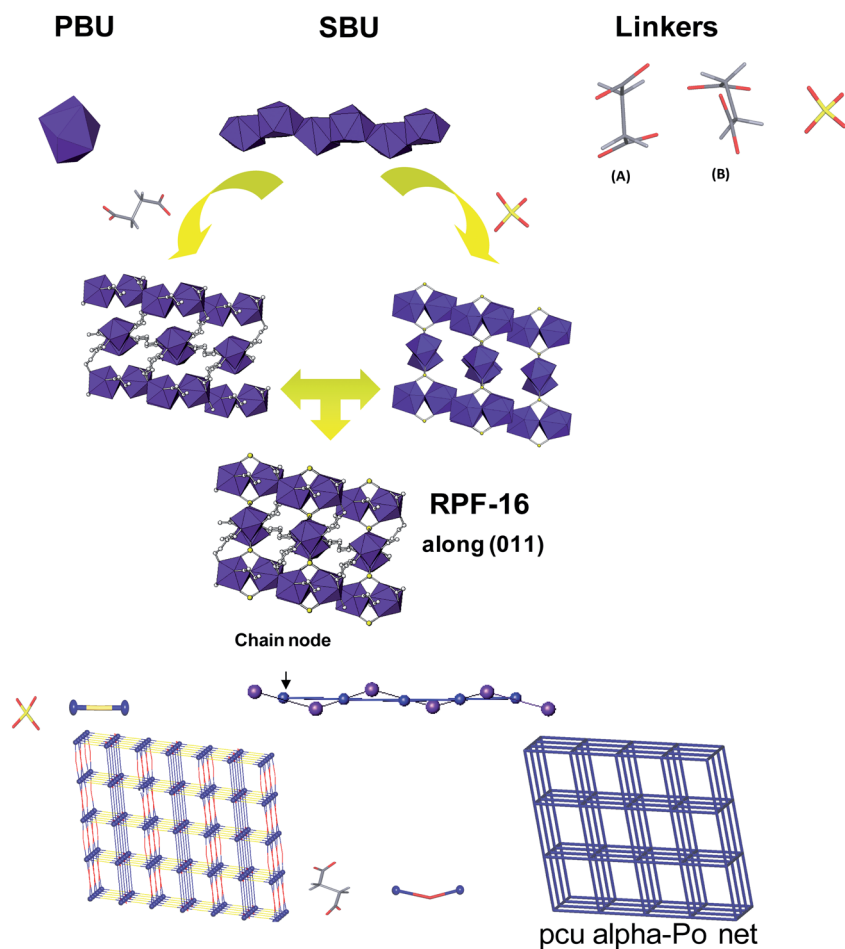


**Fig. 2** Representation of: (up) primary building unit (PBU), secondary building unit, and linkers; (middle) structure formation; (down) schematic description of the 4-connected net ( $4^{12} \times 6^3$ ) topology in **RPF-16**.

$[(\text{LnO})_2\text{SO}_4]$  (ICSD 66823),<sup>26</sup> confirmed in all the cases by X-ray powder diffraction of the TG residue.

compounds are good catalysts if the Ln coordination number is eight or lower, no matter either the kind of lanthanide present or the existence of potentially displaceable coordinated water

### IR spectra

The FT-IR spectra of all **RPF-16** show the same profile (Fig. 4a). The O–H vibration of the coordination water can be identified as one broad and asymmetrical band that involves two components centred at  $\sim 3400$  and  $\sim 3255$   $\text{cm}^{-1}$ , belonging to the two coordination water molecules. Two low intensity bands located at  $\sim 1662$  and  $\sim 1675$  are associated with the water bending vibration mode. The band sited at  $1530$ – $1565$   $\text{cm}^{-1}$  is assigned to  $\nu_{\text{as}}(\text{OCO})$  and the band at  $1328$   $\text{cm}^{-1}$  is associated with  $\nu_{\text{s}}(\text{OCO})$  mode.

The absence of COOH bands indicates that the initial succinic acid is not present in the final product. Low intensity bands corresponding to S–O vibration of the sulfate anion appear in the region of  $1000$ – $942$   $\text{cm}^{-1}$  ( $942$ ,  $957$ ,  $985$  and  $1000$   $\text{cm}^{-1}$ ).

### Catalytic properties

From previous catalytic studies of Ln sulfonate MOFs, which presented both redox and acid sites, we learnt that in those reactions, whose mechanism implies the approximation of the intermediate species to the lanthanide coordination sphere, the

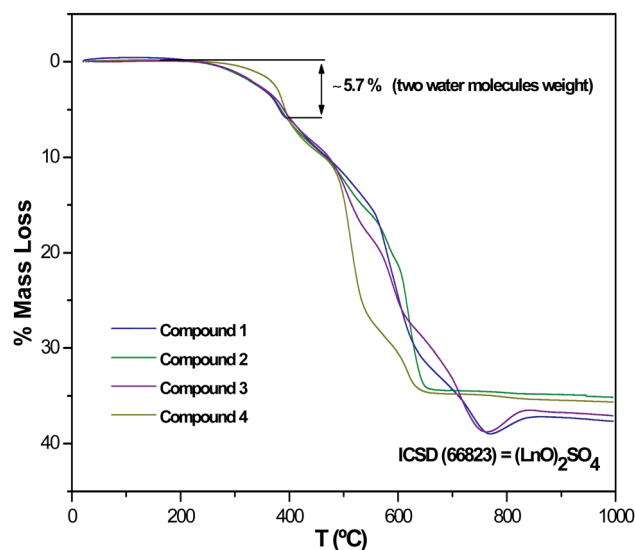


**Fig. 3** TGA of compounds **1–4**, where the decomposition products are  $[(\text{LnO})_2\text{SO}_4]$  (Ln = La, Pr, Nd, and Sm).



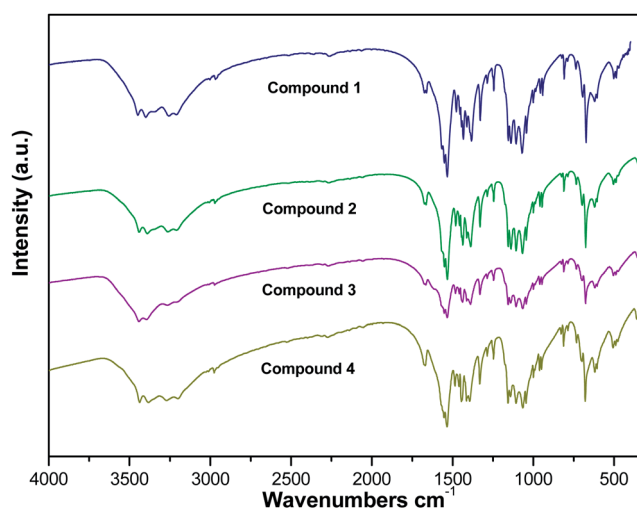


Fig. 4 FT-IR for compounds RPF-16.

molecules. Examples of such reactions, in which the bifunctional character of the materials as catalyst has been tested, are the transformation of linalool,<sup>27,28</sup> or the sulfide oxidation.<sup>7,8,29</sup> In order to confirm this fact, the **RPF-16** materials were used as catalysts in these reactions. As was expected, since the Ln coordination number in these materials is nine, none of the compounds were active as catalysts in these reactions.

A mechanism for the lanthanide MOF-mediated hydrogenation, based on the H<sub>2</sub> heterolytic cleavage, could be analogous to that proposed in which the catalytic activity is explained by the formation of metal-hydride intermediate species. Thinking of a better approximation of the small H<sub>2</sub> molecule to a nine-coordinated lanthanide ion followed by the water molecule displacement, the new series of catalysts was tested for hydrogenation of nitroaromatics.

Nitroaromatics are very important in industry, since these compounds are good starting products due to easy introduction of the nitro group in the aromatic ring. The reduction of simple nitro compounds is readily carried out with various commercially available products<sup>30</sup> (supported copper, cobalt, palladium and nickel). In MOF materials, to our knowledge, only one based on In<sup>31</sup> has been tested in this reaction. With the new **RPF-16** we want to explore, the selective reduction of a nitro group with H<sub>2</sub>, when other reducible groups are present in the same molecule. Functionalized anilines are important intermediates for agrochemicals, pharmaceuticals, dyestuffs, urethanes and other industrially important products and fine chemicals,<sup>32–34</sup> and there is a strong incentive to develop chemoselective catalysts for the reduction of nitro groups.

In this sense, our aim was to test the capacity of the rare-earth MOFs to promote the hydrogenation of nitroaromatics as a heterogeneous catalyst. The first step was to find the conditions under which the compounds were active; different conditions were tested (temperature, hydrogen pressure and catalyst amount). It was observed that the compounds were only active at 363 K at  $5 \times 10^5$  Pa of H<sub>2</sub> pressure in toluene as solvent. The results are presented in Table 2. Compound **1** showed the lowest activity with a TOF value of 29.7 h<sup>−1</sup>. Compounds **2**, **3** and **4** were more active as catalysts. Reactions were carried out with

Table 2 Hydrogenation of nitrobenzene for compounds 1–4

Compound	Yield <sup>a</sup> (%) (h)	TOF <sup>b</sup> /h <sup>−1</sup>
<b>1</b> <sup>c</sup>	100 (6)	29.7
<b>2</b> <sup>d</sup>	100 (1.5)	175.2
<b>3</b> <sup>d</sup>	100 (2)	161.2
<b>4</b> <sup>d</sup>	100 (1.5)	146.8
2 <sup>nd</sup> cycle <sup>de</sup>	100 (2)	126.1
3 <sup>rd</sup> cycle <sup>de</sup>	100 (2.5)	134
4 <sup>th</sup> cycle <sup>de</sup>	100 (2.5)	94

<sup>a</sup> Yield determined by GC-MS. <sup>b</sup> TOF: mmol of substrate/mmol cat. H.

<sup>c</sup> Reaction performed with 1 mol% cat. <sup>d</sup> Reaction performed at 0.5 mol % cat. <sup>e</sup> Compound **2**.

a catalyst/substrate ratio of 1/200 (0.5 mol% catalyst), and compounds **2–4** showed a higher activity than **1**, with TOF values of  $\sim 10^2$  (Table 2). This behaviour is in accordance with the significant difference in the Lewis acidity of the corresponding Ln–metal [La(III) vs. Pr(III), Nd(III) and Sm(III)].<sup>35</sup> This hydrogenation reaction is favoured by the presence of acid centres, because they promote the heterolytic rupture of the hydrogen molecule to form an Ln–hydride intermediate and then the interaction with the substrate (nitro group).<sup>36–39</sup> Fig. 5 shows the kinetic profile for the Ln-catalyzed hydrogenation of nitrobenzene; as can be seen the activity increases in the order La  $\ll$  Sm < Nd < Pr, which is in agreement with the increasing of their Lewis acidity.<sup>35,36</sup>

Under the optimized reaction conditions, the scope of the reaction was explored with structurally and electronically different nitroarenes (Table 3). Substrates with electron-donor (–NH<sub>2</sub> and –CH<sub>2</sub>CN) and electron-acceptor groups (–CHO, Br and I) were tested. In fact, the selective reduction of the nitro groups is practically independent of the substitute. The amines are obtained with high selectivity and at conversion levels about

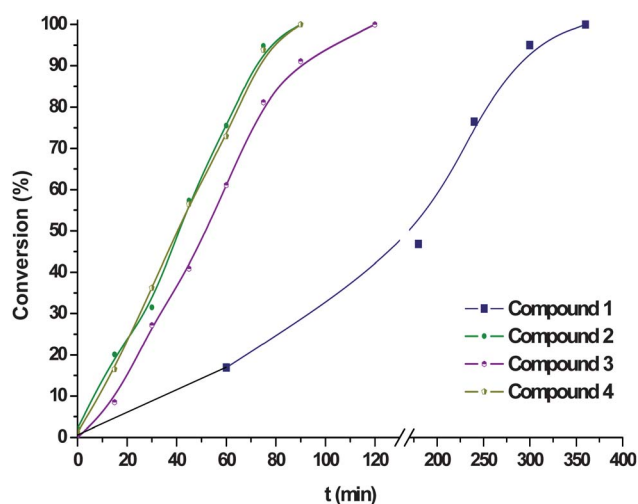
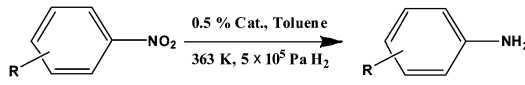
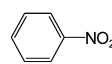
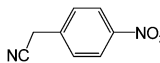
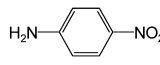
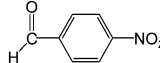
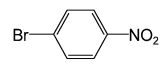
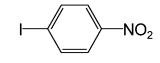


Fig. 5 Kinetic profile for compound (1–4)-catalyzed hydrogenation of nitrobenzene.

**Table 3** Hydrogenation of *para*-nitroarenes for compound **2**

		
Substrate	Yield <sup>a</sup> (%) (h)	TOF <sup>b</sup> /h <sup>-1</sup>
	100 (1.5)	175.2
	100 (1.5)	147.3
	100 (5)	232.0
	100 (1.5)	200.7
	60.5 (5)	29.4
	100 <sup>c</sup> (22)	10.8

<sup>a</sup> Yield determined by GC-MS. <sup>b</sup> TOF: mmol of substrate/mmol cat. H. <sup>c</sup> 30% of nitrobenzene and 70% of aniline were formed.

100%. Dehalogenation was only observed for 4-iodo-nitrobenzene.<sup>40</sup>

### Recycling of catalysts

The heterogeneity of the catalyst is also evaluated to study whether, using compound **2** as catalyst, the reaction occurred on the solid or was catalyzed by species in the liquid phase. To address this issue, we conducted two separate experiments. In the first experiment, the reaction was concluded after 1 h, and the conversion of nitrobenzene was found to be ~60%. At this stage, the catalyst was separated from the reaction mixture and the reaction was continued with the filtrate for an additional 3 h and the conversion remained almost unchanged. In a second experiment, the solid recovered was used again in another reaction by adding new reagents and as shown in Fig. 6 catalytic activity remains unaltered.

Ln catalysts could be recovered for recycling, and reused retaining most of their catalytic activity, and the activity of the recovered catalyst does not decrease after four cycles at least. Analyses of the reused catalysts, separated from the reaction media, showed that the overall catalyst structure was largely maintained (Fig. 6 and Table 3).

We evaluate also the possible bifunctional character of **RPF-16** for the one-pot reductive amination of carbonyl compounds (Scheme 1) because we expected that the Lewis acid character of these compounds may favour the acid-catalyzed step of the reaction. To check this hypothesis, compound **2** was tested as a catalyst for the reaction between nitrobenzene and heptanal. Nitrobenzene is first hydrogenated into the corresponding amines, which can be condensed with heptanal in a second step to yield *N*-heptylideneaniline; this imine is subsequently reduced to

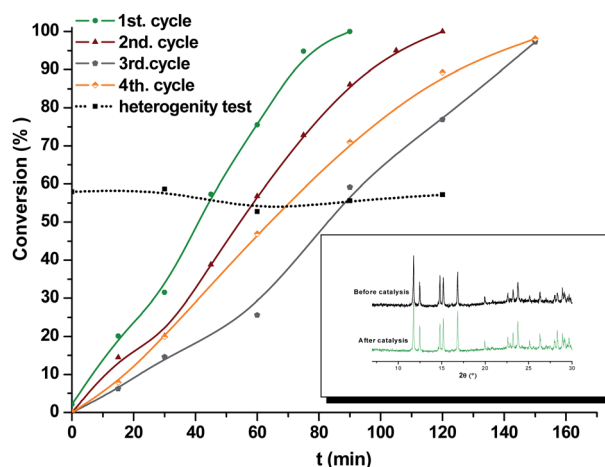


**Fig. 6** Kinetic profile in four consecutive reaction cycles employing compound **2** as a catalyst, the test of solubility of the catalyst and the X-ray powder pattern before and after catalysis.

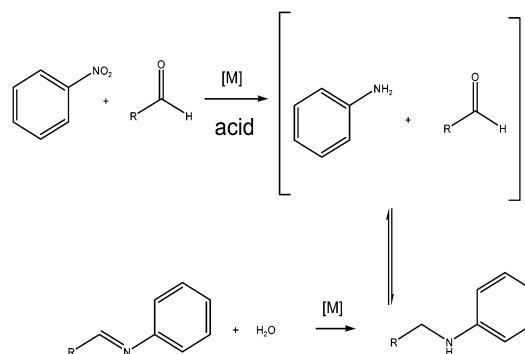
the corresponding secondary amine (*N*-heptylaniline). Fig. 7 shows the kinetic profile for this reaction.

The reaction rate with the current catalyst is lower than with In-MOF<sup>31</sup> (yield 100%, 0.1% catalyst, 4 hours, 40 °C, ethanol). These results can be explained on the basis of the relative acidity of the metallic ions. In being the most acidic, the relative order with the lanthanide in **RPF-16** is La  $\ll$  Pr < Nd < Sm  $\ll$  In.<sup>35</sup>

All in all, **RPF-16** hydrogenates selectively the NO<sub>2</sub> group in the presence of other reducible groups in the same molecule.

### Luminescence measurements

We give now a general overview of the room-temperature luminescence behaviour of the new **RPF-16** Ln materials (Fig. 8). An intense Raman band associated with C–H vibrations (Raman shift around 3000 cm<sup>-1</sup>) overlaps with the emission spectra. There is no emission band that could be associated with the ligand. The Pr-compound shows a narrow band at 608 nm corresponding to the <sup>1</sup>D<sub>2</sub> → <sup>3</sup>H<sub>4</sub>, and a well-split band around 640 nm given by the <sup>3</sup>P<sub>0</sub> → <sup>3</sup>H<sub>6</sub> transition. The bands observed in the high-energy side of the 608 nm band are Raman vibrations also observed in the other compounds. The spectrum of the Nd-compound shows several bands in the range 850–920 nm associated with the <sup>4</sup>F<sub>3/2</sub> → <sup>4</sup>I<sub>9/2</sub> transition. The Sm-compound presents the strongest emission (an order of magnitude higher



**Scheme 1** One-pot synthesis of substituted aromatic amines.

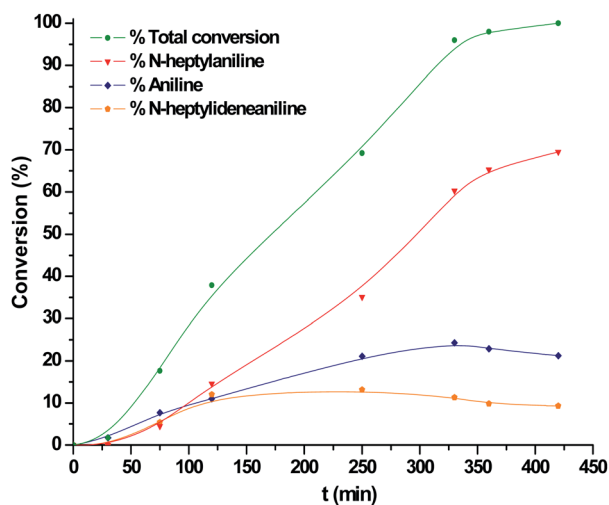


Fig. 7 Kinetic profile for the one-pot reductive amination of heptanal.

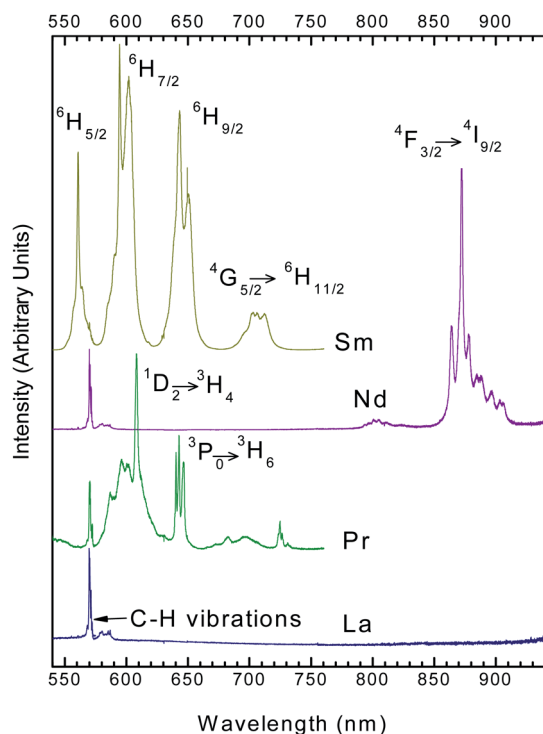


Fig. 8 Room-temperature emission spectra of the RPF-16 compounds at 488 nm excitation.

than that of Pr) composed of several broad bands centered at 560 nm, 600 nm, 645 nm and 710 nm given by the radiative decay from the  $^4G_{5/2}$  level to the  $^6H_{5/2}$ ,  $^6H_{7/2}$ ,  $^6H_{9/2}$  and  $^6H_{11/2}$  levels, respectively.

## Conclusions

The first series of mixed succinate/sulfate/Ln MOFs  $[Ln_2(C_2H_4C_2O_4)_2(SO_4)(H_2O)_2]$  (RPF-16), where Ln = La, Pr, Nd, and Sm, were hydrothermally obtained and their structures determined by X-ray single crystal diffraction. Topological

simplification of RPF-16 isostructural frameworks gives rise to a 3D uninodal six connected net of type **pcu alpha-Po** primitive cubic. Nitro groups of different compounds with carbonyl, nitrile or halide groups have been successfully hydrogenated with RPF-16 as catalysts. The used Ln-MOFs RPF-16 show high chemoselectivity towards reduction of the nitro group at near-complete conversion of the substrate; these catalysts can be used in successive cycles. The bifunctional character for one-pot reductive amination of carbonyl compounds was tested and confirmed. Room-temperature luminescence measurements show that the Sm-compound presents the strongest emission (an order of magnitude higher than that of Pr) of the series.

## Abbreviations

MOF	Metal Organic Framework
RPF-16	Rare-earth Polymer Framework
Succ	Succinate

## Acknowledgements

The authors thank A. E. Platero-Prats for her comments on the topological studies. R.D. acknowledges a FPI scholarship from Spanish Ministry of Science and Innovation (MICIN), and Fondo Social Europeo from the EU. This work has been supported by the Spanish MCYT Project Mat 2007-60822 FAMA and Consolider-Ingenio CSD2006-2001. S.A.G. thanks the CSIC for a postdoctoral contract (Program JAE-DOC).

## References

- 1 J. C. G. Bünzli and C. Piguet, *Chem. Soc. Rev.*, 2005, **34**, 1048.
- 2 J. Rocha, L. D. Carlos, F. A. A. Paz and D. Ananias, *Chem. Soc. Rev.*, 2011, **40**, 926.
- 3 T.-H. Tran-Thi, R. Dagnelie, S. Crunaire and L. Nicole, *Chem. Soc. Rev.*, 2011, **40**, 621.
- 4 G. Férey, C. Serre, T. Devic, G. Maurin, H. Jobic, P. L. Llewellyn, G. De Weireld, A. Vimont, M. Daturi and J.-S. Chang, *Chem. Soc. Rev.*, 2011, **40**, 550.
- 5 H. B. Zhang, C. B. Tian, S. T. Wu, J. D. Lin, Z. H. Li and S. W. Du, *J. Mol. Struct.*, 2011, **985**, 355.
- 6 M. C. Bernini, E. V. Brusau, G. E. Narda, G. E. Echeverria, C. G. Pozzi, G. Punte and C. W. Lehmann, *Eur. J. Inorg. Chem.*, 2007, **2007**, 684.
- 7 F. Gándara, J. Perles, N. Snejko, M. Iglesias, B. Gómez-Lor, E. Gutiérrez-Puebla and M. Á. Monge, *Angew. Chem., Int. Ed.*, 2006, **45**, 7998.
- 8 F. Gándara, E. Gutiérrez-Puebla, M. Iglesias, D. M. Proserpio, N. Snejko and M. A. Monge, *Chem. Mater.*, 2009, **21**, 655.
- 9 A. Corma, H. García and F. X. Llabrés i Xamena, *Chem. Rev.*, 2010, **110**, 4606.
- 10 R. C. Huxford, J. Della Rocca and W. Lin, *Curr. Opin. Chem. Biol.*, 2010, **14**, 262.
- 11 A. Monge, F. Gándara, E. Gutiérrez-Puebla and N. Snejko, *CrystEngComm*, 2011, **13**, 5031.
- 12 R. Sen, S. Koner, D. K. Hazra, M. Helliwell and M. Mukherjee, *Eur. J. Inorg. Chem.*, 2011, 241.
- 13 F. Gándara, A. d. Andrés, B. Gómez-Lor, E. Gutiérrez-Puebla, M. Iglesias, M. A. Monge, D. M. Proserpio and N. Snejko, *Cryst. Growth Des.*, 2008, **8**, 378.
- 14 J. Perles, N. Snejko, M. Iglesias and M. A. Monge, *J. Mater. Chem.*, 2009, **19**, 6504.
- 15 C. N. R. Rao, J. N. Behera and M. Dan, *Chem. Soc. Rev.*, 2006, **35**, 375.

- 16 C. Cascales, B. Gómez-Lor, E. Gutiérrez-Puebla, M. Iglesias, M. A. Monge, C. Ruiz-Valero and N. Snejko, *Chem. Mater.*, 2004, **16**, 4144.
- 17 J. Perles, C. Fortes-Revilla, E. Gutiérrez-Puebla, M. Iglesias, M. A. Monge, C. Ruiz-Valero and N. Snejko, *Chem. Mater.*, 2005, **17**, 2701.
- 18 L. Li, R. Yu, D. Wang, X. Lai, D. Mao and M. Yang, *Inorg. Chem. Commun.*, 2010, **13**, 831.
- 19 Y.-P. Yuan, J.-L. Song and J.-G. Mao, *Inorg. Chem. Commun.*, 2004, **7**, 24.
- 20 H.-C. Liu, I. H. Chen, A. Huang, S.-C. Huang and K.-F. Hsu, *Dalton Trans.*, 2009, 3447.
- 21 Bruker-Siemens, *I.*, V 5.04 ed., Madison, WI.
- 22 Bruker-Siemens, *I.*, V 6.28A ed., Madison, WI.
- 23 Bruker-Siemens, *I.*, V 5.1 ed., Madison, WI.
- 24 N. L. Rosi, J. Kim, M. Eddaoudi, B. Chen, M. O'Keeffe and O. M. Yaghi, *J. Am. Chem. Soc.*, 2005, **127**, 1504.
- 25 V. A. Blatov and D. M. Proserpio, V4.0 ed., Samara, Russia, 2010.
- 26 S. G. Zhukov, A. Yatsenko, V. V. Chernyshev, V. Trunov, E. Tserkovnaya, O. Antson, J. Hoelsae, P. Baules and H. Schenk, *Mater. Res. Bull.*, 1997, **32**, 43.
- 27 N. Snejko, C. Cascales, B. Gómez-Lor, E. Gutiérrez-Puebla, M. Iglesias, C. Ruiz-Valero and M. A. Monge, *Chem. Commun.*, 2002, 1366.
- 28 F. Gándara, A. García-Cortés, C. Cascales, B. Gómez-Lor, E. Gutiérrez-Puebla, M. Iglesias, A. Monge and N. Snejko, *Inorg. Chem.*, 2007, **46**, 3475.
- 29 F. Gándara, E. Gutiérrez-Puebla, M. Iglesias, N. Snejko and M. A. Monge, *Cryst. Growth Des.*, 2009, **10**, 128.
- 30 *Ullmanns Encyclopedia of Industrial Chemistry*, ed. G. Booth, Wiley-VCH Verlag, Weinheim, 2002.
- 31 B. Gomez-Lor, E. Gutiérrez-Puebla, M. Iglesias, M. A. Monge, C. Ruiz-Valero and N. Snejko, *Inorg. Chem.*, 2002, **41**, 2429.
- 32 S. C. Mitchell and R. H. Waring, *Ullmanns Encyclopedia of Industrial Chemistry*, Wiley-VCH Verlag, Weinheim, Germany, 2000.
- 33 B. Coq and F. Figueras, *J. Mol. Catal. A: Chem.*, 2001, **173**, 117.
- 34 F. Figueras and B. Coq, *J. Mol. Catal. A: Chem.*, 2001, **173**, 223.
- 35 N. C. Jeong, J. S. Lee, E. L. Tae, Y. J. Lee and K. B. Yoon, *Angew. Chem., Int. Ed.*, 2008, **47**, 10128.
- 36 G. Jeske, H. Lauke, H. Mauermann, H. Schumann and T. J. Marks, *J. Am. Chem. Soc.*, 1985, **107**, 8111.
- 37 G. Jeske, H. Lauke, H. Mauermann, P. N. Swepston, H. Schumann and T. J. Marks, *J. Am. Chem. Soc.*, 1985, **107**, 8091.
- 38 X. Han, R. Zhou, G. Lai, B. Yue and X. Zheng, *Catal. Lett.*, 2003, **89**, 255.
- 39 Q. Xu, X.-M. Liu, J.-R. Chen, R.-X. Li and X.-J. Li, *J. Mol. Catal. A: Chem.*, 2006, **260**, 299.
- 40 R. Crook, J. Deering, S. J. Fussell, A. M. Happe and S. Mulvihill, *Tetrahedron Lett.*, 2010, **51**, 5181.